

Thermal stability of a fully printed ultra-thin organic pre-amplifier circuit meant for on-skin applications

Aregaw Kujansuu¹, Rei Shiwaku², Tomohito Sekine², Hiroyuki Matsui², Shizuo Tokito², Matti Mäntysalo¹, Mika-Matti Laurila¹

¹Tampere University, Korkeakoulunkatu 3, 33720, Tampere, Finland

²Research Center for Organic Electronics, Yamagata University, Yonezawa 992-8510, Japan

Abstract—We report thermal stability measurement results for a fully printed ultra-thin ($t = 1\mu\text{m}$) organic dual-use pre-amplifier circuit meant for on-skin applications. The pre-amplifier consists of 3 TFTs based on organic small molecule semiconductor polystyrene,2,7-dihexyl-dithieno[2,3-d;2',3'-d']benzo[1,2-b;4,5-b']dithiophene (PS:DTBDT-C6), bias and feedback resistor based on poly(3-hexylthiophene) (P3HT) and printed feedback capacitor. The temperature dependency of the amplifier gain and threshold voltage (V_{th}) are measured in wide range of temperatures (21 to 60 °C). In this temperature range the gain and V_{th} are observed to decrease 1,5 and 1 V, respectively. However, in the real use environment (attached on-skin) the expected temperature changes are significantly smaller because the ultra-thin pre-amplifier can use the body as a natural cooling system: although the ambient temperature may increase even 50 °C, the expected temperature change on the device is only 6 °C and the changes in gain and V_{th} fall to neglectable level (0.24 and 0.18 V, respectively).

Keywords—printed electronics, organic TFTs, temperature stability, ultra-thin devices

I. INTRODUCTION

Ultra-thin printed electronic devices have been recently proposed as a way to implement systems for unobtrusive on-skin monitoring of bio-signals [1][2][3][4]. As these devices are meant to be worn continuously, it is important to ensure that the devices remain operational during the every-day activities which may contain situations where the devices come under significant heat stress. An extreme example of such a situation is a visit to Finnish sauna, where the temperature regularly exceeds 60 °C [5]. However, even in such an extreme situation, the body's thermoregulation system efficiently cools down the skin so that the body may expel the excess heat and retain proper function of the vital organs [5][6]. Now, if an electronic device without active cooling is placed on the skin, the bottom side of the device will have temperature close to the skin temperature whereas the top side temperature will depend on the thermal resistance of the device (R) which, in turn, depends on the material's thermal conductivity (k) and its thickness (t) according to $R = t/k$ [7]. Following the above example of a Finnish sauna, this would mean that a thick enough device has such a high R that its top surface is going to experience the full 60 °C whereas an ultra-thin electronic device of only few μm thickness will be able to utilize the body's natural

cooling system more efficiently and thus keep the device temperature close to the well-regulated skin temperature.

This effect of natural cooling is especially important when the ultra-thin on-skin device contains a pre-amplifier element consisting of thin film transistors (TFTs) fabricated using organic thiophene based semiconducting materials. For example, it has been previously observed that the threshold voltage of P3HT and 6T based TFTs depend significantly on the device temperature [8][9] while the field effect mobility has been observed to be also affected [10][11]. While these studies provide an important window into the physics of the TFT thermal stability, it is equally important to understand the effect of temperature on the performance of an entire operational amplifier unit consisting of multiple such TFTs. Especially as the solution processed devices in general, and printed devices in particular, may suffer from relatively high TFT-to-TFT performance variation.

To shed some light on this issue, we have characterized the thermal stability of a fully printed ultra-thin ($t = 1\mu\text{m}$) organic dual use (charge amplifier or inverter) pre-amplifier circuit consisting of 3 TFTs based on DTBDT-C6 organic semiconductor channel, a P3HT based bias and feedback resistor and a feedback capacitor. The circuit is meant to be used as a preamplifier in continuously worn on-skin bio-signal measurement device and thus the temperature dependency of the amplification and threshold voltage was measured in a wide range of potential temperatures experienced by the user (21 to 60 °C). Significant changes in threshold voltage and lesser changes in amplification were observed within this range. However, we show that the true temperature change of the device in even extreme environments is far smaller due to the thin form factor of the device and thus the shifts in these parameters fall to acceptable levels. Based on this, we hypothesize that even a visit to a Finnish sauna is not beyond the operational range of our devices (at least as far as thermal stress is concerned).

II. MATERIALS AND METHODS

A. Device fabrication

The fully printed dual use (charge amplifier or inverter; see inset of Figure 1 A for circuit diagram) pre-amplifier circuit was fabricated as described in [3], but the main process steps are also described here for convenience: 1) Teflon release layer coating on glass carrier; 2) $1\mu\text{m}$ Parylene-C coating; 3) inkjet printing of 1st metallization layer (e.g. gate, capacitor bottom electrode) using Ag-nanoparticle ink; 4) 150 nm Parylene-C coating for TFT gate and capacitor dielectric; 5) inkjet printing of 2nd metallization

The work of M.M.L. was supported by H2020 Marie Skłodowska Curie Actions (MSCA) Individual Fellowship (IF) Grant UNOPIEZO (Grant no. 10102243) and KAUTE "Tutkijat maailmalle" -program through W.Ahlström Foundation. Work was also supported by Academy of Finland (Grants 353219, 320019, 310617 and 310618)

layer (e.g. gate s/d, capacitor top electrode, resistor electrodes) using Ag-nanoparticle ink; 6) surface treatment with pentafluorobenzenethiol (PFBT); 7) dispensing Teflon surface energy patterns to contain spreading of semiconducting ink in next step; 7) dispensing P3HT for bias resistor and DTBDT-C6 for TFT; 8) dispensing Teflon passivation on top of P3HT and DTBDT-C6.

B. Thermal stability measurements

The voltage transfer curves (VTC) of two samples were measured at temperatures of 21, 30, 35, 40, 45, 50, 55 and 60 °C using the setup described in Figure 1. The electrical characterization part of the setup consisted of an oscilloscope (3000A, Keysight) which was used to monitor the output of the organic amplifier while applying the input signal with an arbitrary waveform generator (33512B, Keysight) and supply voltage with DC power supply (E3640A, Agilent); a custom buffer amplifier was used between the oscilloscope and organic amplifier for impedance matching. The heat control part of the setup consisted of a Peltier element placed underneath the sample while a DC power supply (E3640A, Agilent) was used to power the Peltier element and a laser thermometer to monitor the temperature of the sample's top surface. The VTC measurement data was then post-processed with Matlab to remove 50 Hz noise using a Savitzky-Golay and 1D median filters. Matlab was also used to calculate and plot the derivative of the output voltage as a function of the input voltage to determine the amplifier gain and threshold voltage (V_{th}). The V_{th} was determined as the V_{in} at peak gain. The measurements were performed twice for two samples and only the measurements done with rising V_{in} were included in the analysis.

III. RESULTS AND DISCUSSION

A. Temperature dependency of gain and threshold voltage

The voltage transfer characteristic (VTC) curves for one of the measurement sets performed for Sample 2 are shown in Figure 1 A and the gain calculated based on the VTCs in Figure 1 B.

The average gain and V_{th} values for both samples were extracted from the VTC and gain measurements and they are collected in Figure 2 A and B, respectively. Both gain and V_{th} decrease significantly as the temperature is increased from 21 to 60 °C: gain decreases on average 1.5 while the V_{th} decreases 1 V. The decreasing gain can be explained by temperature dependent change in the feedback resistor value: the P3HT field effect mobility increases with increasing temperature [10][11] and this reduces the voltage drop ($V_{in} - V_{out}$) over the inverter. Similarly, the increased temperature facilitates charge carrier hopping [12][13] in the DTBDT-C6 channel material and a smaller V_{in} is required to draw charge carriers into the channel thereby decreasing the V_{th} . The effect of thermal expansion of Parylene-C gate dielectric can be neglected due to relatively narrow temperature range and the effect of the feedback capacitance can be neglected due to the low V_{in} sweep frequency (10 mHz).

Although the absolute value of gain and V_{th} differ sample-to-sample, the slope of the linear fit reveals that they both follow the same trend (see Table 1). Furthermore, the high coefficient of determination indicates that the linear fit may be used to predict the gain and V_{th} at different temperatures.

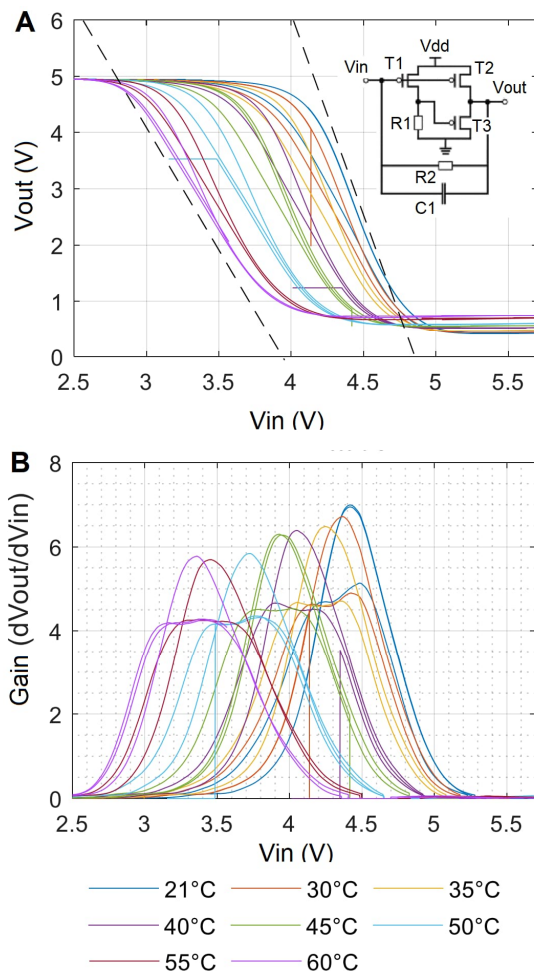


Figure 1: A) Voltage transfer characteristic (VTC) curves at various temperatures for Sample 2 (inset shows the circuit diagram) and B) gain calculated based on the VTC curves. The VTC were measured with increasing V_{in} (higher peaks) and decreasing V_{in} (lower peaks); only the measurements done with increasing V_{in} were used in further analysis.

Table 1: Parameters for linear fit ($y = a + b \cdot x$) in Figure 2. R^2 indicates the coefficient of determination.

	Sample1 Gain	Sample2 Gain	Sample1 V_{th}	Sample 2 V_{th}
a	11.37	7.76	5.5	5.16
b	-0.04	-0.04	-0.03	-0.03
R^2	0.68	0.93	0.97	0.96

B. Body as a natural cooling system for ultra-thin devices

As mentioned in the introduction, the body's thermoregulation system keeps the skin temperature in a very narrow range even in the most extreme environments and the ultra-thin devices are able to utilize this natural cooling system much more effectively when compared to thick devices due to their lower thermal resistance. To illustrate this effect, a simple heat transfer problem is solved to estimate the top surface temperature of our device in a 60 °C environment (see Figure 3).

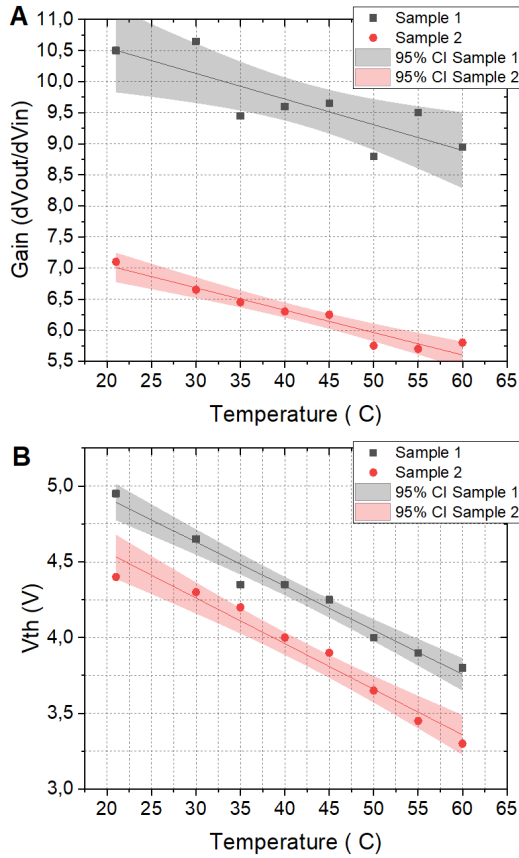


Figure 2: A) Gain vs. temperature and B) threshold voltage (V_{th}) vs. temperature measured with increasing V_{in} (see Figure 1 caption). The gray and red shadow area indicate the 95% confidence interval for the linear fit.

Air	$T_{air} = 60\text{ }^{\circ}\text{C}$ $h = 15\text{ W/m}^2\text{K}$	
Parylene-C	$k = 0.08368\text{ W/m}^{\circ}\text{K}$ $t = 1\text{ }\mu\text{m}$	$T_{top} = ???$
Skin	$T_{skin} = 34.5\text{ }^{\circ}\text{C}$	

Figure 3: Thermal parameters for determining the devices top surface temperature in hot environment [6][14][15].

The bottom side of the device is assumed to have the same temperature as the skin i.e. $34.5\text{ }^{\circ}\text{C}$ [6]. In thermal equilibrium, the convective heat transfer on air – Parylene-C interface (Q_{conv}) equals the conductive heat transfer on skin – Parylene C interface (Q_{cond}):

$$Q_{cond} = Q_{conv} \rightarrow -k \cdot A \cdot (T_{top} - T_{skin}) / t = h \cdot A \cdot (T_{top} - T_{air}) \quad (1)$$

where k is the thermal conductivity of Parylene C, A the area of the sample, T_{top} the top surface temperature of the Parylene C, T_{skin} the skin temperature, t the thickness of the sample, h the convective heat transfer coefficient of air and T_{air} the air temperature. Solving the equation (1) for T_{top} yields:

$$T_{top} = (-t \cdot h \cdot T_{air} - k \cdot T_{skin}) / (-k - t \cdot h) \quad (2)$$

Solving this equation with the parameters given in Figure 3 reveals that even in a $60\text{ }^{\circ}\text{C}$ environment the difference between the skin and the top surface of the device is neglectable (34.500 vs. $34.505\text{ }^{\circ}\text{C}$, respectively). The top surface temperature is also plotted as a function of the device

thickness in Figure 4 A to illustrate the importance of minimizing the device thickness to efficiently utilize the body's thermoregulation system for device cooling. Figure 4 B shows that the convective heat transfer coefficient (h) of ambient environment has neglectable effect on top surface temperature (c.f. the h for air in free convection is between 0.25 and $25\text{ W/m}^2\text{K}$, while in forced convection it may be up to $500\text{ W/m}^2\text{K}$ [15]).

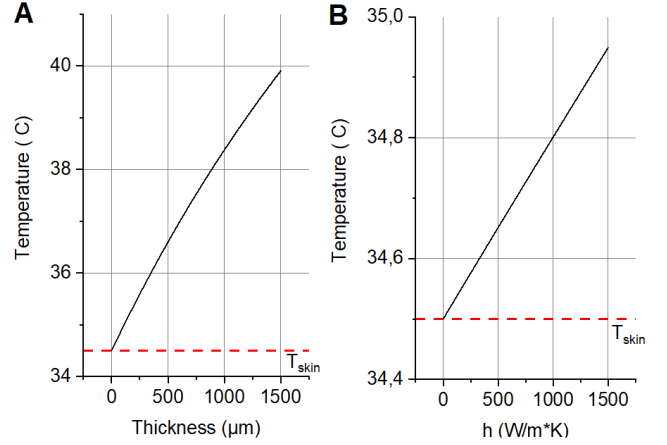


Figure 4: Top surface temperature of the device in situation depicted in Figure 3 as function of A) the device thickness and B) the convective heat transfer coefficient of ambient environment

We may now re-consider the temperature range which the device is subject to during every-day activities. The difference in average skin temperature before and after 10 minute visit to $70\text{ }^{\circ}\text{C}$ sauna has been measured to be only $6\text{ }^{\circ}\text{C}$ (rising from ~ 34 to $\sim 40\text{ }^{\circ}\text{C}$ [5][6]) and based on the above consideration, the pre-amplifier temperature will follow this trend with neglectable difference. Using regression equations for gain and V_{th} from Table 1 we may calculate that the expected maximum temperature change of $6\text{ }^{\circ}\text{C}$ will result in only 0.24 shift in the gain and 0.18 V shift in the V_{th} . Both values are neglectable which indicates that the operation of the pre-amplifier is not significantly altered even during such extreme ambient temperature changes because the ultra-thin device is able to use the body as a natural cooling system.

IV. CONCLUSION

Temperature dependency of gain and threshold voltage of a fully printed ultra-thin pre-amplifier circuit was investigated. Because the ultra-thin form factor allows the device to use the body as natural cooling system, the temperature changes experienced by the pre-amplifier are significantly smaller than the temperature changes in ambient environment. This results in very small expected changes in the gain and threshold voltage of the pre-amplifier when attached on the skin.

ACKNOWLEDGMENT

The authors thank the Tosoh Corporation for providing the semiconductor material DTBBDT-C6.

REFERENCES

- [1] K. Lozano Montero et al., "Self-Powered, Ultrathin, and Transparent Printed Pressure Sensor for Biosignal Monitoring," *ACS Appl. Electr. Mat.*, vol. 3, no. 10, pp. 4362–4375, Oct. 2021.
- [2] M.-M. Laurila et al., "Self-powered, high sensitivity printed e-tattoo sensor for unobtrusive arterial pulse wave monitoring," *Nano Energy*, vol. 102, p. 107625, Nov. 2022
- [3] M.-M. Laurila et al., "A Fully Printed Ultra-Thin Charge Amplifier for On-Skin Biosignal Measurements", *IEEE Journ. Electr. Dev. Soc.*, vol. 7, pp. 566 – 574, May 2019
- [4] C. Dagdeviren et al., "Conformable amplified lead zirconate titanate sensors with enhanced piezoelectric response for cutaneous pressure monitoring", *Nat. Comm.*, vol. 5, p. 4496, Aug. 2014
- [5] J. Leppäluoto, "Human thermoregulation in sauna", *Ann. Clin. Res.*, vol. 20, no. 4, pp. 240-243, Jan. 1988
- [6] B. Vainer, "FPA-based infrared thermography as applied to the study of cutaneous perspiration and stimulated vascular response in humans", *Phys. Med. Biol.*, vol. 50, pp. 63-94, Nov. 2005
- [7] P. Böckh et al., *Heat Transfer*, 1st ed., Springer: Heidelberg, 2012
- [8] E.J. Meijer et al., "Switch-on voltage in disordered organic field-effect transistors", *Appl. Phys. Lett.*, vol. 80, no. 20, pp. 3838-3840, May 2002
- [9] G. Horowitz et al., "Temperature and gate voltage dependence of hole mobility in polycrystalline oligothiophene thin film transistors", *Journ. Appl. Phys.*, vol. 87, no. 9, pp. 4456-4463, May 2000
- [10] S. Joshi et al., "Bimodal Temperature Behavior of Structure and Mobility in High Molecular Weight P3HT Thin Films", *Macromol.*, vol. 42, pp. 4651-4660, May 2009
- [11] C. Liu et al., "Anisotropic conductivity–temperature characteristic of solution-cast poly(3-hexylthiophene) films", *Synth. Met.*, vol. 156, pp. 1362-1367, Dec. 2006
- [12] F. M. Li, *Organic thin film transistor integration a hybrid approach*. Weinheim: Wiley-VCH, 2011
- [13] P. Stallinga, *Electrical Characterization of Organic Electronic Materials and Devices*, 1st ed.. Chichester, UK: John Wiley & Sons Ltd, 2009.
- [14] "Parylene Thermal Characteristics", *Advanced Coating Inc.*, [WWW]: <https://www.advancedcoating.com/thermal-properties>, Accessed: 26.10.2022
- [15] P. Kosky et al., *Exploring engineering*, 2nd ed., Elsevier: Burlington, MA, USA, 2010